

STUDY OF QUASI-PERIODIC VARIATIONS IN DRAG OF ARTIFICIAL SATELLITE DURING 23–24 SOLAR CYCLES

Komendant V.H.¹, Ryabov M.I.², Sukharev A.L.²

¹Astronomy Department of Odessa I.I.Mechnikov National University

²Odessa observatory «URAN-4» Institute of Radio Astronomy NASU

ABSTRACT. Apply of the method of time-frequency analysis allows to reveal the detailed structure of the manifestations of the influence of the state space weather on the upper atmosphere of the Earth. Sensitive indicators of such changes are low-orbit satellites. The dynamics of drag of nineteen low-orbit satellites was viewed. The study period includes phases of declining and a long minimum of 23rd solar cycle, phases of rise and maximum of 24th solar cycle. In dynamic of inhibition of all the analyzed satellite pronounced regular inhibition effects with extended periods of 2 – 6 years and short-period effects with periods less than one year. In the satellites: 00063, 00165, 25064, 00932 and 00746 – detected periods with trend from 25 – 28 days to 1 – 1.7 months.

1. Introduction

In this work, satellites are used as indicators of the impact of space weather and manifestations of solar activity on the upper atmosphere of the Earth. Density variations cause a change in the height of the satellite in the atmosphere. The density of the atmosphere is constantly changing and doesn't only depend on the latitude and height above the Earth's surface, but also on the solar activities and space weather conditions. Evolution of the orbit and drag of satellites depends on: gravitational and tidal perturbations (the attraction of the Sun, Moon and other planets); compression of the Earth; the Earth's magnetic field; light pressure; charged and neutral particles (the effect is small and therefore neglected); aerodynamic disturbances of Earth atmosphere [1, 2].

2. Observational data

Nineteen satellites with different inclinations were taken for the analysis. Among them: polar, middle-latitude and equatorial satellites. There are nine circle orbit and ten elliptic orbit satellites. Some elements of the orbits of this satellites are listed in Table 1. In brackets (after number of satellite) period of observation of the satellite is shown.

Most of all satellites were observed during 10 years. Satellite 27700 was observed during 8 years (2005 – 2012). Observations of these satellites cover the declining phase of solar cycle 23 and the first half of solar cycle 24. It includes the rise phase and beginning of the maximum phase of solar cycle 24.

In Table 1 are listed: numbers of satellites, periods of observations, inclination of orbits – i , eccentricity – e and the minimum distance from the surface of the Earth at perigee – r_{min} .

Table 1.

Number of satellite	i	e	r_{min}
satellites with circular orbit			
25860 (2005-2013)	98.57°	0.0002	655 km
27700 (2005-2012)	97.7°	0.005	486 km
12054 (2005-2013)	65°	0.007	522 km
00397 (2005-2014)	58.3°	0.0016	613 km
00063 (2005-2014)	48.5°	0.0027	465 km
00165 (2005-2014)	47.9°	0.0013	540 km
06153 (2005-2014)	35°	0.00077	697 km
25064 (2005-2013)	34.9°	0.0007	507 km
23757 (2005-2013)	22.9°	0.0009	499 km
satellites with elliptical orbit			
00932 (2005-2014)	81.3°	0.114	522 km
00721 (2005-2014)	78.6°	0.11	592 km
00829 (2005-2014)	60.8°	0.3	393 km
00746 (2005-2014)	60.8°	0.31	399 km
00082 (2005-2014)	38.9°	0.12	631 km
00016 (2005-2014)	34.3°	0.2	649 km
00005 (2005-2014)	34.2°	0.19	647 km
00020 (2005-2014)	33.4°	0.17	505 km
00011 (2005-2014)	32.9°	0.15	551 km
00963 (2005-2014)	19.75°	0.21	265 km

3. Initial values

Variations of the B-star Drag Term were studied in this article. This Drag Term strongly correlates with the density of the atmosphere. In this case, it can be seen as drag coefficient. The B-star Drag Term is used for the model SGP 4. This mathematical model is used for prediction of the position and velocity of an artificial satellite (there are 5 mathematical model of SGP) [7]. This model uses TLE data format produced by NORAD – North American Aerospace Defense Command [5]. The B-star Drag Term measured in units of $1/R_3$ (R_3 – radius of the Earth).

4. Methods of data processing

Packages of the statistical analysis were used for our estimations, which are: Origin Pro 8.1, STATISTICA 8 и PSELab.

For primary processing of data software package – Origin Pro 8.1 was used. With it performed data interpolation by B-spline method and subtracted the trend (polynomial 3rd order and using of frequency filtering). After this package statistical analysis software package STATISTICA 8 was used. With this package periodograms for all satellites were constructed. At the last stage the PSELab package was used for construction of the spectrograms. PSELab allows to carry out the spectral and spectral–time analysis of data.

5. Application of spectral analysis of time series

Spectral analysis is one of the signal processing methods, which allows to describe the frequency content of the measured signal. The basis for this analysis is the Fourier transform. It binds the values of the time series with their representation in the frequency domain.

The disadvantage of this method is that it can't show the period of time when the amplitude of any harmonic changes. One option to eliminate this disadvantage was proposed. It is based on using the method not to the entire process, but to the process within a certain time window, which gradually shifts [3]. To recalculate the coefficients of the resulting series we used the algorithm of fast Fourier transform (FFT). In this work, for construction of the spectrograms we used algorithm "Winograd". This algorithm has a significant advantage over the others, when the multiplication operation is more difficult than addition [4].

6. Results

Due to the fact that the data series are presented on an uneven timeline, to create a time series with uniform samples we used the B-spline interpolation. Figure 1 shows an example graph of the change of the drag coefficient of the satellites: 27700, 00932 – in the investigated time interval.

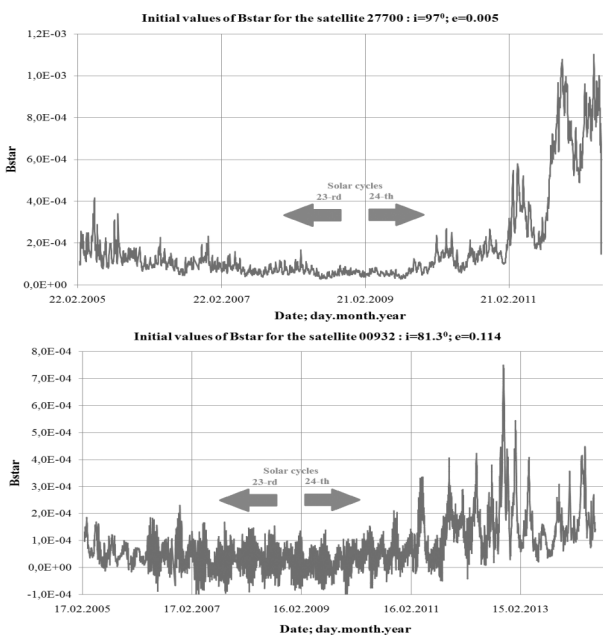


Figure 1: Initial values for polar satellites 27700 (circular orbit) and 00932 (elliptical orbit).

Fig. 1 shows a marked difference in the drag dynamics of the satellites at period of the minimum of the 23rd solar cycle and at the beginning of the 24th solar cycle.

As a result of the carried out calculations we obtained that there are quasi-periodic oscillations with an interval of 27 to 30 days in the declining phase of the 23rd solar cycle and in the phase of minimum solar activity. On this oscillations overlaid the oscillations with period of 10 to 13 days. In addition to these observations drags with a period of slowdown of about three months are marked.

6.1. Dividing the data into two intervals of observations

According to the drag dynamic of the artificial satellites, marked above, observations data was divided into two periods: 2005-2009 and 2010-2014. In STATISTICA 8, using Fourier analysis, we constructed periodograms for these intervals. An example of periodogram is shown in Figure 2.

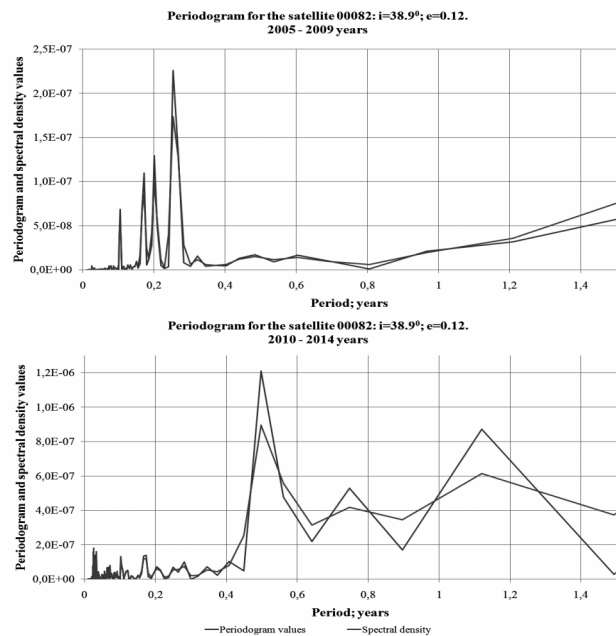


Figure 2: Periodogram of initial values for two time periods (satellite 00082).

In the resulting periodograms: for 2005 – 2009 dominated periods of up to 0,5 years. And for 2010–2014 we see increasing of period 0,5 year and manifestation of longer periods of 1 – 1,2 years («elliptic» satellites) and 2,4 year («circular» satellites). For all objects in the declining phase of the 23rd solar cycle, the maximum amplitude has a short–period variations (up to 0,5 year), in the raise phase of the 24th solar cycle the maximum amplitude has the long–period variations (from 0,5 year to 2,5 years).

6.2. Subtract of the trend component

Table 2 lists the periods of trend component. It shows existence of six years period and about two–year period. All of them have maximum spectral power. Further, to identify short–components, trend components were removed.

Table 2.

Number of satellite	Periods; Year - *, Months - **, Days - ***.		
satellites with circular orbit			
25860 $i=97.7^\circ$	6*	2*	11,1**
27700 $i=97^\circ$	1,7*	1,1*	6,6**
12054 $i=65^\circ$	6*	3*	1*
00397 $i=58.3^\circ$	6,4*	2,1*	1,1*
00063 $i=48.5^\circ$	2,1*	1,3*	8,9**
00165 $i=47.9^\circ$	2*	11,3**	8,6**
06153 $i=35^\circ$	6,4*	2,1*	1,1*
25064 $i=34.9^\circ$	2*	11,1**	8**
23757 $i=22.9^\circ$	6*	2*	11,1**
satellites with elliptical orbit			
00932 $i=81.3^\circ$	6,4*	1,8**	1,3**
00721 $i=78.6^\circ$	6,4*	2,1*	1,1*
00829 $i=60.8^\circ$	6,4*	2,1*	11,7**
00746 $i=60.8^\circ$	2,1*	1,3*	11,8**
00082 $i=38.9^\circ$	6,4*	1,6*	11,7**
00016 $i=34.3^\circ$	2,5*	11,7**	8*
00005 $i=34.2^\circ$	6,4*	2,1*	11,7**
00020 $i=33.4^\circ$	1,3*	8**	5,9**
00011 $i=32.9^\circ$	6,4*	2,1*	1,1*
00963 $i=19.75^\circ$	6,4*	2,1*	11,7**

Table 3.

Number of satellite	Periods; Year - *, Months - **, Days - ***.								
satellites with circular orbit									
25860 $i=97.7^\circ$	2,4*	1*	8**	6**	3,5**	26,2***			
27700 $i=97^\circ$	2,47*	1,7*	9,9**	6,6**	5,9**	4**	1,8**	27,6***	
12054 $i=65^\circ$	2*	1*	8,5**	6**	5**	3,6**	2,5**	27,3***	
00397 $i=58.3^\circ$	2,5*	1,1*	8,5**	5,9**	4,1**	1,2**	25,9***	10,9***	
00063 $i=48.5^\circ$	2,5*	1,2*	9,4**	6**	4**	1,8**	27***		
00165 $i=47.9^\circ$	2,4*	1*	8,2**	6,1**	3,3**	27,4***			
06153 $i=35^\circ$	2,1*	11,7**	8,5**	5,9**	4**	1,4**	25,6***	9,6***	F
25064 $i=34.9^\circ$	2*	1*	8**	6**	3,5**	1,7**	27,3***		
23757 $i=22.9^\circ$	2*	1*	8**	6**	4**	27,3***			
satellites with elliptical orbit									
00932 $i=81.3^\circ$	1,3*	11,8**	9,5**	5,9**	2,9**	1,5**	27,2***	12,9***	
00721 $i=78.6^\circ$	1,8*	1,1*	8,4**	5,9**	4**	2,9**	12,7***		
00829 $i=60.8^\circ$	1,8*	11,7**	9**	5,7**	4,6**	2,3**	1,6**		
00746 $i=60.8^\circ$	1,8*	11,8**	8,5**	5,7**	21,5***				
00082 $i=38.9^\circ$	2,5*	1,1*	6,1**	3,1**	2,5**	2**	1,2**	26***	9***
00016 $i=34.3^\circ$	1,8*	11,7**	6,1**	3,6**	2,8**	2,3**	1,5**	11,2***	
00005 $i=34.2^\circ$	1,8*	6,1**	4,9**	3,4**	2,2**	25,5***	11***		
00020 $i=33.4^\circ$	1,3*	8**	6**	4,4**	1,2**	25,8***			
00011 $i=32.9^\circ$	1,1*	6,1**	4,1**	2,5**	25,5***				
00963 $i=19.75^\circ$	1,8*	11,7**	6,1**	3,4**	1,8**	26,8***	9***		

F – faint period

In order to eliminate the influence of the trend components we subtracted the 3rd order polynomial. Then frequency filtering of periodicities more than three years was conducted.

As a result of calculations in Fig. 3 we found periods of 9 – 12,7 days and 1,3 – 2,5 years. For the elliptic orbit satellites periods of: 1 year; 1,8 years and 2,5 years. For the circle orbit satellites periods of: 1 year; 1,2 years; 2,4 – 2,5 years.

6.3. Calculations of the spectrograms for data with subtracted trend

To identify the time of existence of periodic components the program PSELab was used [6]. The result of its application to the Equatorial satellite 25064 is shown in Figure 4.

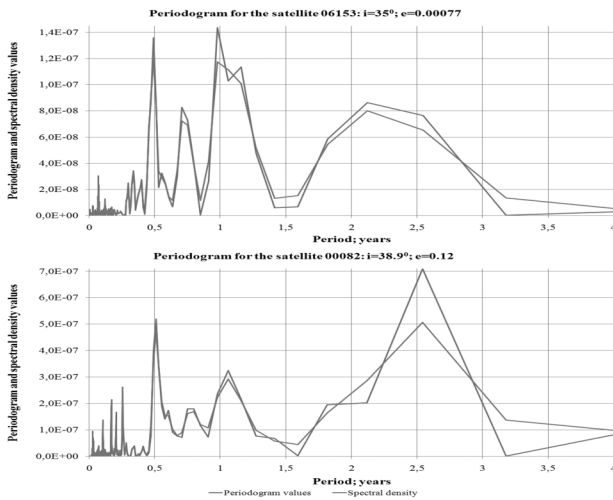


Figure 3: Periodograms with subtracted trend for satellites: 06153 and 00082.

Table 3 shows periods of «circular» and «elliptic» satellites after subtract of the trend components. It lists periods from 2,5 years to 3 months that have maximum spectral power, and periods of less than one month with less spectral power. There are: around annual, semiannual and 27 day periodicities for the «circular» and «elliptic» satellites. For the «circular» satellites we found periods of 2 – 2,5 years and for the «elliptic» satellites – near to biennial periods.

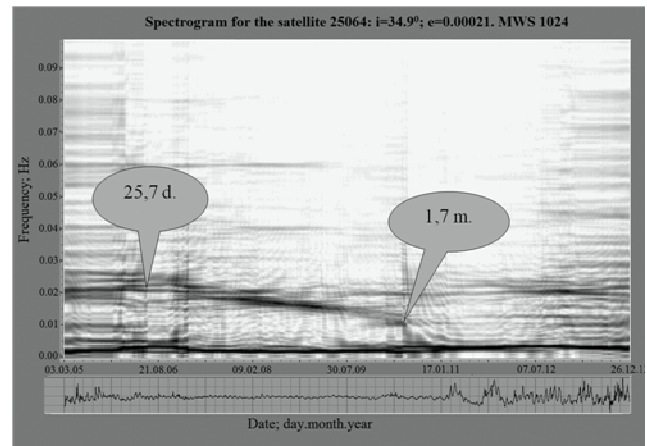


Figure 4: Spectrogram for the Equatorial satellite 25064.

In Figure 4 marked period with trend from 25,7 days to 1,7 month. For satellites: 00063, 00165, 25064, 00932 and 00746 – detected periods with trend from 25 – 28 days to 1 – 1,7 month, and for the satellite 00165 – from 6,4 to 7,2 days.

Table 4.

Number of satellite	Periods: Year - *, Months - **, Days - ***.						
satellites with circular orbit							
25060 $\varphi=97.7^\circ$	1,2 ^A	5,6 ^{**} G/F on D,M	26,2 ^{***} F on A	14,7 ^{***} F on D,M	3,6 ^{***} F on D,M		
27700 $\varphi=9^\circ$	1,2 ^A	6,4 ^{**} G/FT on D,M	26,1 ^{***} F on A	13,5 ^{***} F on A	9 ^{***} F on D,M		
12064 $\varphi=48^\circ$	1,4 ^A	5,8 ^{**} G/FT on D,M	2,5 ^{***} F on A	24 ^{***} F on A	13,3 ^{***} F on A	8,5 ^{***} F on D,M	
00397 $\varphi=58,3^\circ$	1,6 ^A	6 ^{**} G/F on D,M	26,1 ^{***} F on A	10,6 ^{***} M/F on D,G	9 ^{***} M		
00063 $\varphi=48,5^\circ$	1,5 ^A	5,9 ^{**} G/FT on D,M	26,2 ^{***} F on A	23,2 \approx 13,7 ^{***} D,M	8,9 ^{***} D		
00165 $\varphi=41,5^\circ$	1,4 ^A	1 ^A G	5,9 ^{**} G/F on D,M	26,2 ^{***} F on A	6,4 \rightarrow 7,2 ^{***} M		
06153 $\varphi=35^\circ$	1,5 ^A	9,1 ^{**} G/FT on D,M	5,9 ^{**} G/F on D,M	2,1 ^{**} D,M	26,2 ^{***} F on A	11,2 ^{***} D,M/F on G	9,3 ^{***} D,M/F on G
25064 $\varphi=34,5^\circ$	1,2 ^A	5,8 ^{**} D,G/F on M	25,7 ^{***} F on A	29,2 \approx 1,2 ^{**} M	9 ^{***} F on D,M		
25757 $\varphi=22,5^\circ$	1,4 ^A	5,7 ^{**} G/F on D,M	26,1 ^{***} F on A	13,5 ^{***} F on D,M	9 ^{***} F on D,M		
satellites with elliptical orbit							
00932 $\varphi=61,3^\circ$	1,3 ^{FT} on A	6,1 ^{**} G/F on D,M	2,9 ^{**} A	25,7 ^{***} F on A	13,9 ^{***} A	10,2 \approx 9,7 ^{***} D,M	2,2 ^{***} A
00721 $\varphi=78,6^\circ$	1,7 ^F on A	9,9 ^{**} A	5,4 ^{**} G/FT on D,M	3,7 ^{**} G/FT on D,M	1,9 ^{**} A	12,6 ^{***} A	11,2 ^{***} A
00829 $\varphi=60,8^\circ$	2,1 ^F on A	5,6 ^{**} A/F on D,M	2,6 \approx 1,3 ^{**} D,M	26,2 ^{***} FT on M	12,3 ^{***} F on A		
00746 $\varphi=60,8^\circ$	1,3 ^{FT} on A	8,6 ^{**} FT on A	8,4 ^{**} A	1 \rightarrow 12,7 ^{***} D,M			
00082 $\varphi=34,5^\circ$	2,5 ^A /F on M	5,8 ^{**} G/F on D,M	3 ^{**} M/FT on G	2,4 ^{**} D/FT on M,G	3 ^{**} F on A	1,2 ^{**} A	11,5 ^{***} G/F on D,M
00016 $\varphi=34,3^\circ$	1,4 ^D /F on M,G	5 ^{**} G	3,5 ^{**} D,M/F on G	2,2 ^{**} F on A	1,4 ^{**} F on A	11,2 ^{***} F on A	
00005 $\varphi=34,2^\circ$	1,8 ^A	1,1 ^A G	5 ^{**} D,G	3,2 ^{**} F on A	2,1 ^{**} F on A	1,4 ^{**} F on A	26,7 ^{***} F on A
00020 $\varphi=33,4^\circ$	1,3 ^A	5,9 ^{**} G/F on D,M	12,6 ^{***} F on D,M	10,7 ^{***} F on D,M			
00011 $\varphi=32,5^\circ$	1,1 ^A	6,1 ^{**} FT on A	25 ^{***} F on A				
00963 $\varphi=19,75^\circ$	1,4 ^{FT} on A	7,3 ^{**} A	2 ^{**} F on A	25,6 ^{***} F on A	9 ^{***} D,M		

F – faint period; FT – fitful period; D – on the declining phase of the 23rd solar cycle; G – on the rise phase of the 23rd solar cycle; M – on the minimum phase; A – on all observation period.

Table 4 shows the most significant periods of spectrograms for all of the objects. The period of about 0,5 years is present on all observation period for all circle orbit satellites. Such period was detected for elliptic orbit satellites. Periods more than one year are present at the entire range of observations not for all satellites.

7. Conclusions

As a result of the calculation using the programs: OriginPro 8.1, STATISTICA 8 and PSELab have been found:

- 1) difference in the drag dynamics of the satellites at the minimum of the 23rd solar cycle and at the beginning and maximum of the 24th solar cycle;
- 2) the offset of maximum amplitude from short-period variations (up to 0,5 year) in the declining phase of the 23rd solar cycle, to the long-period variations (from 0,5 year to 2,5 years) in the raise phase of the 24th solar cycle;
- 3) periods were detected with trend from 25 – 28 days to 1 – 1,7 month, and for the satellite 00165 – from 6,4 to 7,2 days.

Using Fourier analysis identifies short-periodic components from 11 to 14 days for the circle orbit satellites and 12,7 days for the elliptic orbit satellites. Detected periods with trend probably are related to the dynamics of influence of solar and geomagnetic activity and tidal phenomena on the upper atmosphere of the Earth.

The following steps assume the equating of the received data with the manifestations of solar activity and magnetic storms. The purpose of such research is the consideration of various factors in the prediction models of the upper atmosphere of the Earth.

References

1. Beletsky V.V.: 1965, *The motion of an artificial satellite about the center of mass*, M., 416 p.
2. Roy A.: 1981, *Orbital motion*, M.: Mir, 544 p.
3. Marple S.L.: 1990, *Jr. Digital spectral analysis with applications* (Trans. from english), M.: Mir, y., 584 p.
4. Oppenheim A., Schafer R.: 2006, *Digital signal processing*, M.: Technosphere, 856 p.
5. NORAD [web resource] /North American Aerospace Defense Command. Access mode: <http://www.norad.mil/>.
6. PSELab [web resource] /Power Spectrum estimation laboratory, Access mode: <http://pselab.ru/>.
7. Felix R. Hoots, Ronald L. Roehrich. SPACETRACK Report No.3 [web resource] / Models for Propagation of NORAD Element Sets, 1980. Access mode: <https://celestrak.com/NORAD/documentation/spacetrk.pdf>.